Available online at www.sciencedirect.com
ScienceDirect
Thin Solid Films 516 (2008) 3204–3209
www.elsevier.com/locate/tsf

High mobility, transparent, conducting Gd-doped In_2O_3 thin films by pulsed laser deposition

R.K. Gupta [a], K. Ghosh [a], S.R. Mishra [b], P.K. Kahol [a,*]

[a] Department of Physics, Astronomy, and Materials Science, Missouri State University, Springfield, Missouri-65897, USA
[b] Department of Physics, The University of Memphis, Memphis, TN 38152-6670, USA

Received 22 December 2006; received in revised form 23 July 2007; accepted 7 September 2007
Available online 15 September 2007

Abstract

Highly transparent and conducting thin films of gadolinium doped indium oxide, which have high electron mobility, were deposited on quartz substrate to study the effect of growth temperature and oxygen pressure on their structural, optical, and electrical properties. X-ray diffraction study reveals that these films are randomly oriented on the quartz surface. The average particle size of the films grown at 600 °C was calculated to be ~23 nm. The optical transparency of the films increases with an increase in the growth temperature. The film transparency is also found to increase with increased oxygen pressure during deposition. The electrical properties of these films strongly depend on both the growth temperature and the oxygen pressure. Analysis of the electrical data shows that the mobility of the films increases with increase in the growth temperature.

Keywords: Hall effect; Indium oxide; Gadolinium; Laser ablation; Optical properties; Transparent conducting oxide; Mobility

1. Introduction

Transparent conducting oxides (TCO) have lately attracted considerable attention of researchers and opto-electronic industries because of their unique transparent and conducting properties [1–3]. These oxides are widely used in opto-electronic devices such as light emitting diodes, photodetectors, touch panels, flat panel displays, and solar cells [4–6]. High electrical conductivity, high mobility, and good transparency are essential requirements for these devices [7,8]. According to the Drude model, optical transparency depends on the plasma frequency, which shifts to shorter wavelengths with higher carrier concentration [9]. To obtain high transparency and conductivity, one therefore needs to increase the mobility.

Among the various TCO, indium oxide (In_2O_3) doped with tin is widely used because of its low electrical resistivity and high transparency [10]. But the mobility of these films is not very high (29 cm^2/V s). It is observed that doping of indium oxide with molybdenum instead of tin improves the carrier mobility (>70 cm^2/V s) [9]. Titanium doping also improves the mobility of the indium oxide films. Hest et al. [11] deposited titanium doped indium oxide by sputtering and observed a maximum mobility in their experiments of 83.3 cm^2/V s.

Pulsed laser deposition (PLD) has been widely used for the deposition of TCO thin films [12]. PLD technique has several advantages such as: (a) The composition of multicomponents of a target is maintained in the deposited film; (b) The film grown by this technique is very smooth [13]; and (c) This requires lower substrate temperature relative to other physical vapor deposition techniques [1]. Gadolinium oxide (Gd_2O_3) is a rare-earth oxide which is used in electronic devices due to its good electrical, mechanical and optical properties [14]. Dekhel has studied the optical and electrical properties of gadolinium-indium oxide prepared by thermal evaporation [14,15]. To the best of our knowledge, no studies based on electrical, structural, and optical properties of gadolinium-indium oxide have been done using PLD.

In the present communication, we are reporting the deposition and characterization of transparent and conducting indium oxide thin films which were doped with two atomic weight percent of gadolinium. Gadolinium doped indium oxide (GIO) films were deposited by the pulsed laser method. The highest mobility obtained for the film grown under an oxygen pressure of 5.0×10^{-3} Pa (at 400 °C) is 128 cm^2/V s.

* Corresponding author. Tel.: +1 417 836 4467; fax: +1 417 836 6226.
E-mail address: PawanKahol@missouristate.edu (P.K. Kahol).

0040-6090/$ - see front matter © 2007 Elsevier B.V. All rights reserved.
doi:10.1016/j.tsf.2007.09.012

2. Experimental details

A gadolinium doped In_2O_3 target for the pulsed laser deposition was prepared by standard solid-state reaction method using high purity In_2O_3 (99.999%) and Gd_2O_3 (99.999%). Required amounts of In_2O_3 and Gd_2O_3 were taken by molecular weight and mixed thoroughly to get the target of In_2O_3 having two atomic weight percent of gadolinium. The well-ground mixture was heated in air at 850 °C for 12 h with several intermediate grindings. The powder mixture was cold pressed using hydraulic press at 6×10^6 N/m^2 load and sintered in air at 1000 °C for 12 h.

Thin films were deposited on quartz substrate using KrF excimer laser (Lambda Physik COMPex, $\lambda=248$ nm and pulsed duration of 20 ns) under suitable growth conditions such as substrate temperature and oxygen pressure in the PLD chamber. The laser was operated at a pulse rate of 10 Hz, with an energy of 300 mJ/pulse. The laser beam was focused onto a rotating target at a 45° angle of incidence. Thin films were deposited at temperature of room, 200 °C, 400 °C, and 600 °C (under vacuum of base pressure 1.2×10^{-3} Pa) and under oxygen pressures of 1.0×10^{-3} Pa, 5.0×10^{-3} Pa, 1.0×10^{-2} Pa, 5.0×10^{-2} Pa, 1.0×10^{-1} Pa, 1×10^{0} Pa, and 1.0×10^{1} Pa (at substrate temperature of 400 °C). The deposition chamber was initially evacuated to 1.2×10^{-3} Pa and during deposition oxygen gas was introduced into the chamber to obtain the pressures mentioned above. The growth rate for the films was ~3 nm/min.

The structural characterization was performed using X-Ray Diffraction (XRD) and Raman spectroscopy. The XRD spectra of all the films were recorded with Bruker AXS X-ray diffractometer using the $2\theta-\theta$ scan with CuK_α ($\lambda=$ 1.5405 Å) radiation operated at 40 kV and 40 mA. Micro-Raman scattering experiments were performed in perfect backscattering geometry using a fiber-optically coupled confocal micro-Raman system (TRIAX 320) which is equipped with a liquid N_2 cooled charge coupled detector. Atomic force microscopy (AFM) imaging was performed under ambient conditions using a Digital Instruments (Veeco) Dimension-3100 unit with Nanoscope® III controller, operated in tapping mode. The etched silicon tapping tips employed in the study had a nominal apex radius of curvature of ~10–20 nm and a cone angle of ~34°. The spring constant of the cantilever was ~42 N/m. The cantilevered tip was oscillated close to the mechanical resonance frequency of the cantilever (typically, 200–300 kHz) with amplitudes ranging from ~10 to 30 nm. The optical transmittance measurements were made using UV–visible spectrophotometer (Ocean Optics HR4000). Infrared (IR) spectra were recorded using Bruker FT-IR spectrometer (Vertex 70).

The resistivity and Hall coefficient measurements were carried out by a standard four-probe technique. Gold contacts (thickness 150 nm) were used for all electrical measurements. The gold contacts were deposited on the top of the films using a physical mask having four holes (1×1 mm^2) at the corner of square (1×1 cm^2) under vacuum of base pressure 1.2×10^{-3} Pa at room temperature using PLD. The thickness of the films were measured using AFM and is approximately 100 nm. The film resistivities have been determined by taking the product of resistance and film thickness. The Hall effect was measured with the magnetic field applied perpendicular to film surface in the

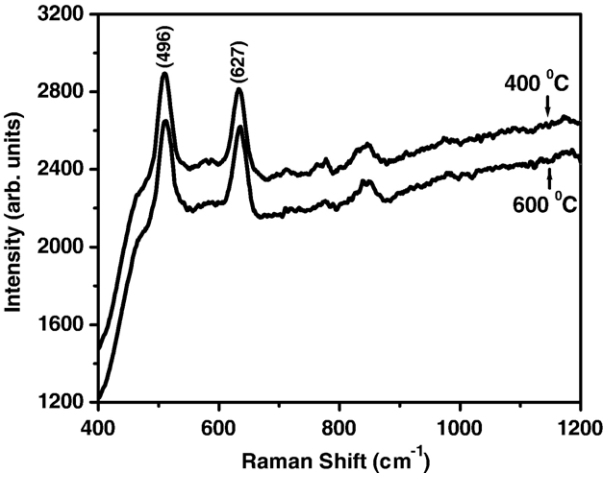

Fig. 2. Raman spectra of GIO thin films grown at different temperatures (in vacuum, base pressure 1.2×10^{-3} Pa).

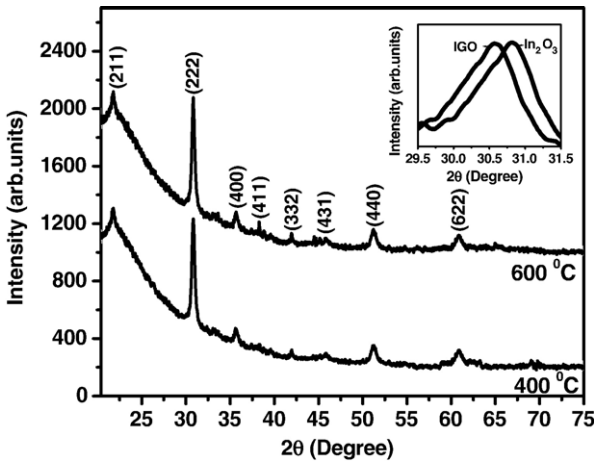

Fig. 1. XRD patterns of GIO film grown at different temperatures (in vacuum, base pressure 1.2×10^{-3} Pa) on quartz substrate.

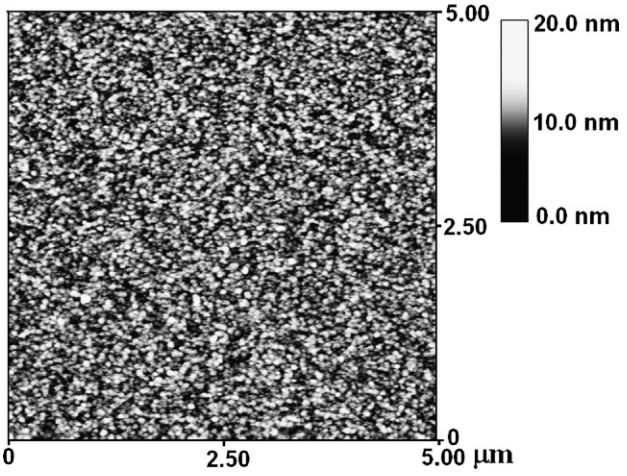

Fig. 3. AFM images of GIO film grown at 400 °C under oxygen pressures of 1×10^{-2} Pa.

Van der Pauw configuration [16]. The Hall voltage is measured by applying magnetic field of ±1.5 T using an electromagnet. The Hall voltage was measured with a nanovoltmeter (model 182, Keithley) with current ranges from +100 to −100 μA using a 20-ppm stable (model 230, Keithley) current source. All the data were collected using an IBM-compatible PC via IEEE-488 interface. The type of the conducting carriers was confirmed to be *n* type for all samples from the observed negative slope in magnetic field versus Hall voltage plots. Carrier concentration and carrier mobility were calculated at room temperature using Hall coefficient and resistivity data [17].

3. Results and discussion

Fig. 1 shows the X-ray diffraction patterns of the thin films of GIO which were grown at different temperatures under vacuum of base pressure 1.2×10^{-3} Pa on quartz substrate. All the peak positions are in good agreement with the JCPDS file card no. 06-0416 for In_2O_3. It is observed that the films are randomly oriented on the quartz substrate. A minor shift in the position of XRD peaks towards lower angles has been observed for GIO compared to In_2O_3. A representative plot of XRD data

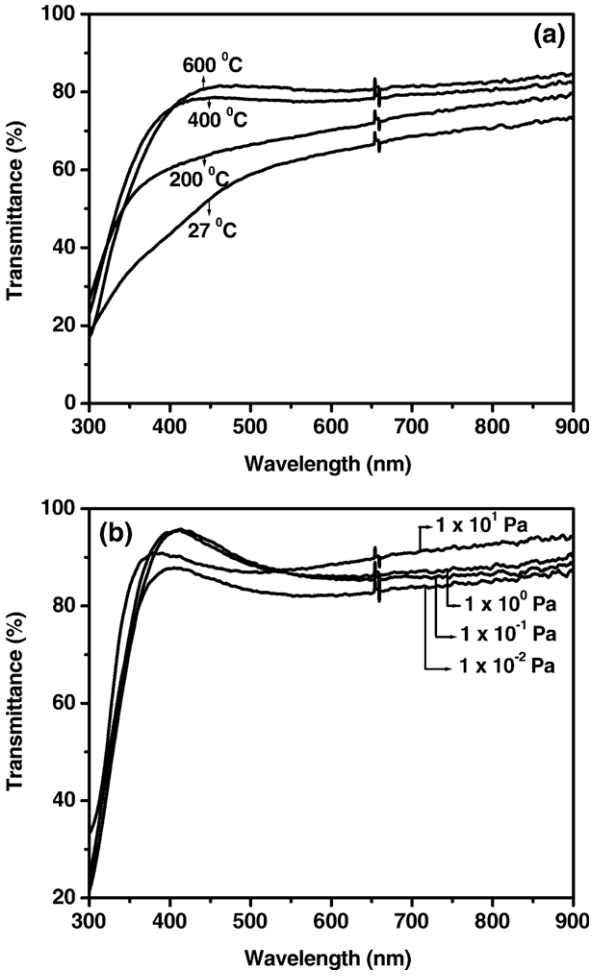

Fig. 4. Transmittance spectra of GIO films grown at (a) different temperatures (in vacuum, base pressure 1.2×10^{-3} Pa) (b) different oxygen pressures (at 400 °C).

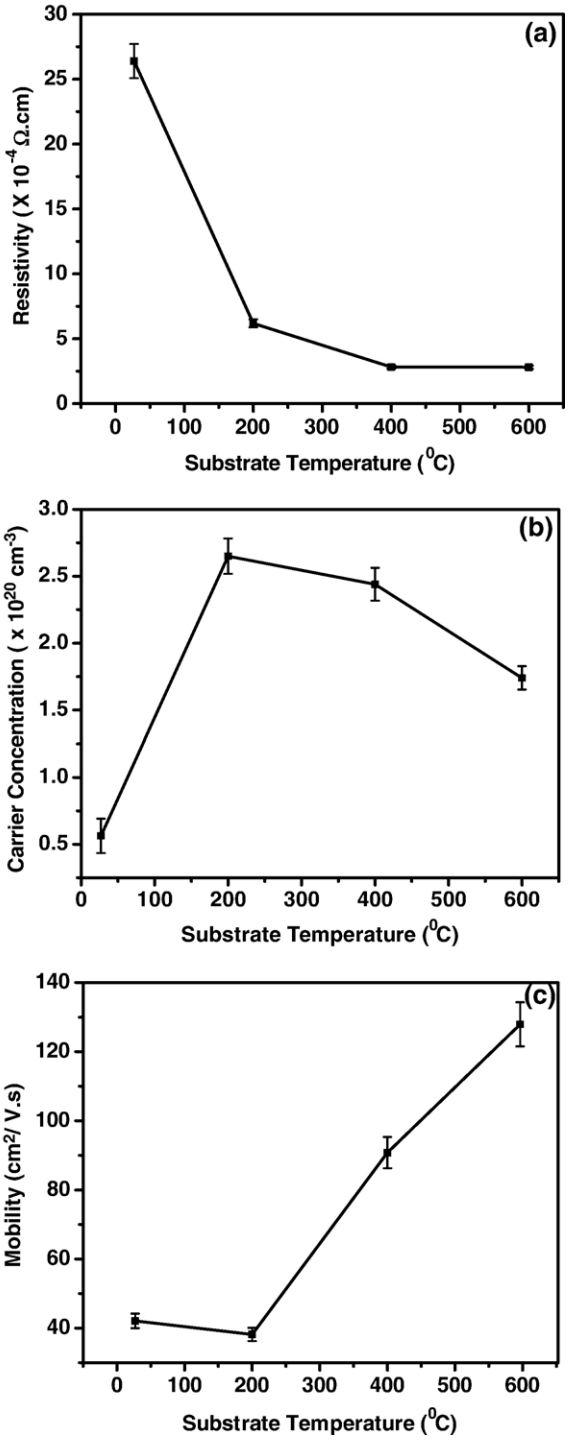

Fig. 5. Effect of substrate temperature on (a) resistivity, (b) carrier concentration, and (c) mobility of GIO films grown under vacuum (base pressure 1.2×10^{-3} Pa).

for In_2O_3 and GIO films grown at identical conditions (under vacuum at 400 °C) are shown in inset of Fig. 1. This result indicates that the lattice is expanding. The increase of lattice constant is obvious as the ionic radius of gadolinium is larger than that of indium. The volume expansion is estimated to be 2.06%. Observation of the volume increase and absence of any impurity peaks suggest gadolinium atom goes to the indium site. That is, the diffractograms provide evidence of single phase crystalline indium oxide (body centered cubic lattice) [18,19].

Table 1
Electronic parameters of GIO grown at different temperature (under vacuum, base pressure 1.2×10^{-3} Pa) on quartz substrate

Temperature (°C)	R_H (cm^3/C)	ρ (Ω cm)	n (cm^{-3})	μ (cm^2/V s)
27	1.11×10^{-1}	2.64×10^{-3}	5.63×10^{19}	4.21×10^{1}
200	2.36×10^{-2}	6.18×10^{-4}	2.65×10^{20}	3.82×10^{1}
400	2.56×10^{-2}	2.82×10^{-4}	2.44×10^{20}	9.08×10^{1}
600	3.59×10^{-2}	2.80×10^{-4}	1.74×10^{20}	1.28×10^{2}

The average particle size of the film grown at 600 °C was calculated using the Scherrer equation [20], and is estimated to be ~23 nm. The Williamson–Hall relationship was used to calculate the lattice distortion ratio (strain) in these films [21]. The percentage strain in the particles grown on the quartz substrate is estimated to be 4.4%. It is observed that as the growth temperature decreases the average grain size also decreases, and the film shows its amorphous nature.

The Raman spectra of the GIO films grown at different temperatures under vacuum are shown in Fig. 2. Characteristic Raman peaks corresponding to indium oxide appeared at 496 and 627 cm^{-1}. The indium oxide belongs to cubic C-type rare-earth oxide structure and for this type of structure the factor group analysis predicts $4A_g$ (Raman)+$4E_g$ (Raman)+$14T_g$ (Raman)+$5A_u$ (inactive)+$5E_u$ (inactive)+16 T_u (infra-red) modes [22]. All the observed modes correspond well to the band positions reported in the literature for cubic indium oxide [23]. Characteristic Raman peaks corresponding to gadolinium oxide is expected at 359, 442 and 565 cm^{-1} [24]. No additional peaks due to the addition of gadolinium are observed. This result indicates once again the absence of any impurity phase due to gadolinium doping in indium oxide.

Fig. 3 shows an AFM image (5×5 μm^2) of a GIO film grown on quartz at 400 °C under an oxygen pressure of 1.0×10^{-2} Pa. The grain size seems to be uniform for the film which is believed to be due to the formation of a solid solution with a crystal structure. The root mean square (rms) value of surface roughness of the GIO film was found to be 1.7 nm, which is much superior than the commercially available indium tin oxide films (~4 nm) [25]. This result shows that our films have highly smooth surface.

The optical transmittance of the GIO films grown under different growth conditions is presented next. It has been observed that the color of the films depends on the growth temperature and oxygen pressure. The films deposited at room temperature are brownish while films deposited at higher growth temperatures become colorless. The dependence of the optical transmittance on growth temperature is shown in Fig. 4 (a). The transparency (color) of the films may be correlated to the degree of crystallinity of the films [26]. The effect of oxygen pressure during growth on the optical transparency of the films is shown in Fig. 4(b). These films are highly transparent. In general, films grown under oxygen atmosphere are more transparent compared with the films grown under vacuum. It is also observed that a good transparent film is obtained when the oxygen pressure is in the range of 1–0.1 Pa.

The effect of substrate temperature (under vacuum of base pressure 1.2×10^{-3} Pa) and oxygen pressure (at substrate temperature of 400 °C) on the electrical properties of GIO thin films are presented next. The carrier concentration (n) is derived from the relation $n=1/e\,R_H$, where R_H is the Hall coefficient and e is the absolute value of the electron charge. The carrier mobility (μ) is determined using the relation $\mu=1/ne\rho$, where ρ is resistivity [17].

Fig. 5(a) shows the dependence of electrical resistivity on substrate temperature. Resistivity decreases continuously with

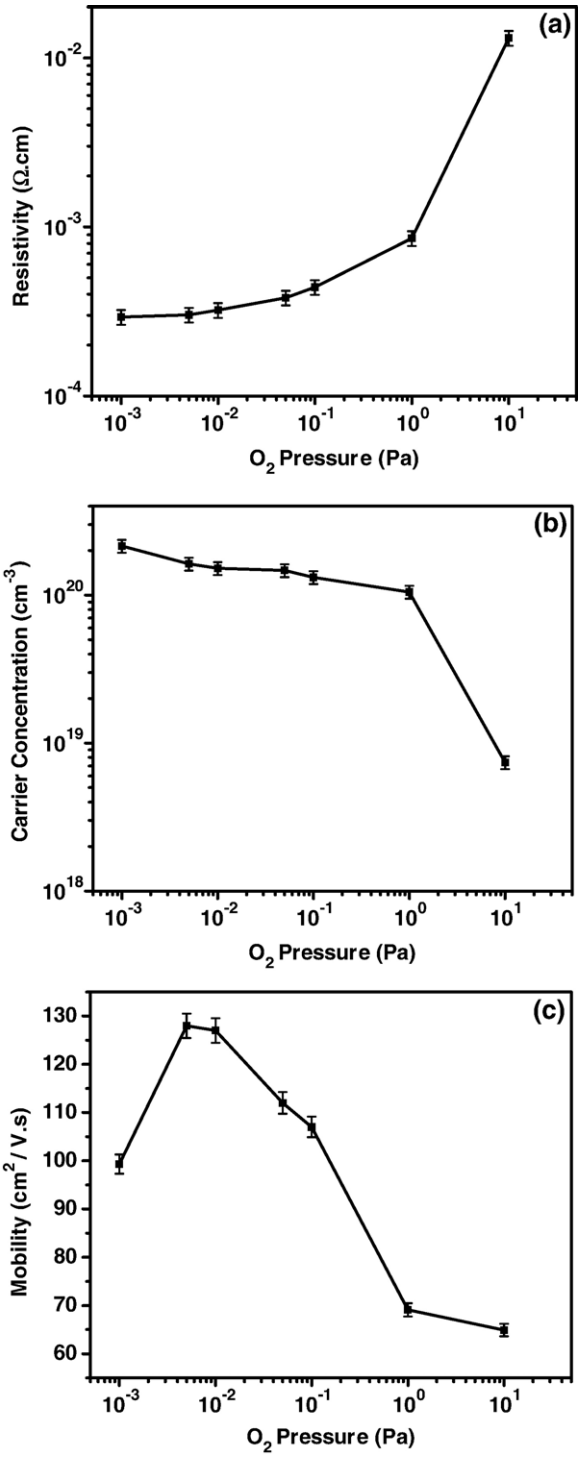

Fig. 6. Effect of oxygen pressure on (a) resistivity, (b) carrier concentration, and (c) mobility of GIO films grown at 400 °C on quartz.

increase in the substrate temperature. The decrease in resistivity with an increase in substrate temperature is believed to be due to improvement in the crystallinity of the films at higher temperatures [1]. This is supported by X-ray diffraction analysis which indicates that the films grown at high temperature are more crystalline and the crystallinity decreases with decrease in growth temperature. The films grown at room temperature were amorphous in nature. The grain size of the films grown at room temperature was ~12 nm, which increased to ~23 nm for the films grown at 600 °C. An increase in grain size with an increase in the substrate temperature leads to reduced grain boundary scattering and thus a decrease in electrical resistivity [1]. The effect of substrate temperature on carrier concentration is shown in Fig. 5(b). It has been observed that the carrier concentration decreases with increase in substrate temperature. The decrease in carrier concentration with temperature may be caused by the extinction of oxygen vacancies from the films at higher temperature [13]. Fig. 5(c) shows the dependence of electron mobility on the growth temperature. The electron mobility continuously increases with increase of the growth temperature. The mobility increases form 38 to 128 cm^2/V s as the growth temperature increases from 200 to 600 °C. The increase in mobility may be due to the better crystallinity of the films, which increases with the increase in substrate temperature. As a result of high mobility, low resistivity at high temperature is observed. Some electrical parameters of the films grown at different temperatures are given in Table 1.

Fig. 6 shows the effect of oxygen pressure on the electrical properties of the GIO films. It is observed that the resistivity, carrier concentration, and mobility are very sensitive to the oxygen pressure. The electrical resistivity of the films, shown in Fig. 6(a), increases with an increase of oxygen pressure in the PLD chamber during film growth, but the carrier concentration decreases with the increase of oxygen pressure. Similar results have been observed by Bellingham et al. for the pure indium oxide and tin doped indium oxide films [27]. The carrier concentration decreases from 2.15×10^{20} to 7.4×10^{18} cm^{-3} as the oxygen pressure increases from 0.001 to 10 Pa. The increase in resistivity with an increase in oxygen pressure can be explained on the basis of oxygen vacancies in the GIO lattice. Increasing oxygen pressure during film growth decreases the number of oxygen vacancies in the deposited films, which leads to decrease in carrier concentration and concomitantly to an increase in film resistivity [13,28]. Fig. 6(c) shows the variation of electron mobility with oxygen pressure. The electron mobility decreases with increase in oxygen pressure in the PLD chamber. The highest mobility observed is 128 cm^2/V s at an oxygen pressure of 5.0×10^{-3} Pa. The low mobility at high oxygen partial pressure was attributed to the excess oxygen acting as scattering centers for free electrons [29]. Electrical parameters of the films grown under different oxygen pressure are given in Table 2.

Table 2
Electronic parameters of GIO grown at different oxygen pressure at 400 °C on quartz substrate

Oxygen pressure (Pa)	R_H (cm^3/C)	ρ (Ω cm)	N (cm^{-3})	μ (cm^2/V s)
–	2.56×10^{-2}	2.82×10^{-4}	2.15×10^{20}	9.08×10^{1}
1.0×10^{-3}	2.91×10^{-2}	2.93×10^{-4}	2.15×10^{20}	9.93×10^{2}
5.0×10^{-3}	3.83×10^{-2}	3.02×10^{-4}	1.63×10^{20}	1.28×10^{2}
1.0×10^{-2}	4.10×10^{-2}	3.22×10^{-4}	1.52×10^{20}	1.27×10^{2}
5.0×10^{-2}	4.25×10^{-2}	3.81×10^{-4}	1.47×10^{20}	1.12×10^{2}
1.0×10^{-1}	4.72×10^{-2}	4.40×10^{-4}	1.32×10^{20}	1.07×10^{2}
1.0×10^{0}	5.93×10^{-2}	8.57×10^{-4}	1.05×10^{20}	6.91×10^{1}
1.0×10^{1}	8.44×10^{-1}	1.31×10^{-2}	7.40×10^{18}	6.49×10^{1}

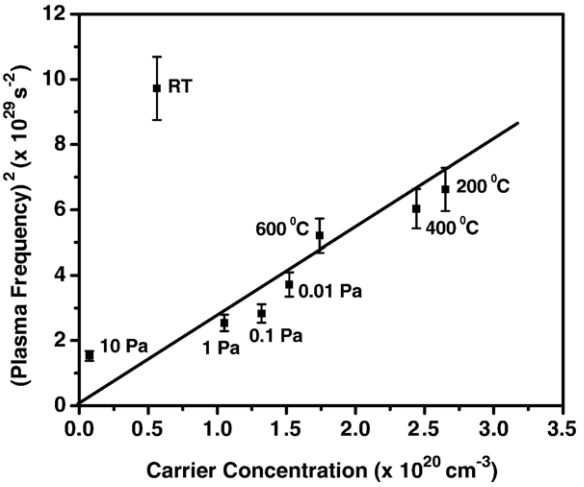

Fig. 7. Effect of variation of carrier concentration on plasma frequency of GIO films grown at different substrate temperature (under vacuum) and under different oxygen pressure (at 400 °C).

The effect of carrier concentration (determined by the Hall effect) on the plasma frequency is presented next. The plasma frequency (ω_p) for all the samples was obtained through IR-Spectroscopy. To check the consistency of our results we analyzed both electrical and optical data through the Drude model, according to which $\omega_p^2=(ne^2/\varepsilon_0 m^*)$, where ε_0 is the free space permittivity, e is the charge of an electron, n is the carrier concentration and m^* is the effective free electron mass, [9]. Fig. 7 shows dependence of the square of plasma frequency on carrier concentration. All the data except room temperature fit well with the Drude model. The deviation form Drude model at room temperature is not very clear at this moment. This may be due to the high resistivity and low transparency of the film grown at room temperature.

4. Conclusions

Highly conducting and transparent gadolinium- doped indium oxide films were grown on quartz substrate using the pulsed laser deposition technique. The growth temperature and the oxygen pressure in the chamber play a significant role in obtaining high mobility films. The electrical properties and optical transparency of the films depend both on growth temperature and oxygen pressure. Our films show highest mobility ever obtained on indium oxide films.

Acknowledgement

The authors are thankful to Erin E. Sutton, Centre for Applied Science and Engineering, Missouri State University,

Missouri for recording the AFM picture. The authors are also thankful to Prof. E. Steinle, Department of Chemistry, Missouri State University, Missouri for recording IR spectra. This work is partially supported by Research Corporation (award number CC6166).

References

[1] H. Kim, J.S. Horwitz, G.P. Kushto, S.B. Qadri, Z.H. Kafafi, D.B. Chrisey, Appl. Phys. Lett. 78 (2001) 1050.
[2] I. Hamberg, C.G. Granqvist, J. Appl. Phys. 60 (1986) R123.
[3] C.G. Granqvist, A. Hultaker, Thin Solid Films 41 (2002) 1.
[4] C.N. Carvalho, G. Lavareda, A. Amaral, O. Conde, A.R. Ramos, J. Non-Cryst. Solids 352 (2006) 2315.
[5] A.V. Singh, R.M. Mehra, J. Appl. Phys. 90 (2001) 5661.
[6] J.H. Lee, S.Y. Lee, B.O. Park, Mater. Sci., Eng., B 127 (2006) 267.
[7] H. Kim, A. Pique, J.S. Horwitz, H. Murata, Z.H. Kafafi, C.M. Gilmore, D.B. Chrisey, Thin Solid Films 377 (2000) 798.
[8] P.F. Newhouse, C.H. Park, D.A. Keszler, J. Tate, P.S. Nyholm, Appl. Phys. Lett. 87 (2005) 112108.
[9] H.F.A.M. Hest, M.S. Dabney, J.D. Perkins, D.S. Ginley, Thin Solids Films 496 (2006) 70.
[10] T. Minami, MRS Bull. 25 (2000) 38.
[11] H.F.A.M. Hest, M.S. Dabney, J.D. Perkins, D.S. Ginley, M.P. Taylor, Appl. Phys. Lett. 87 (2005) 032111.
[12] J.P. Zheng, H.S. Kwok, Appl. Phys. Lett. 63 (1993) 1.
[13] H. Kim, C.M. Gilmore, A. Pique, J.S. Horwitz, H. Mattoussi, H. Murata, Z.H. Kafafi, D.B. Chrisey, Appl. Phys. Lett. 86 (2001) 6451.
[14] A.A. Dakhel, Chem. Phys. Lett. 393 (2004) 528.
[15] A.A. Dakhel, Solid State Electron 49 (2005) 562.
[16] L.J. Van der Pauw, Philips Res. Rep. 13 (1958) 1.
[17] I. Yasuhiro, K. Hirokazu, Appl. Surf. Sci. 169/170 (2001) 508.
[18] P.K. Manoj, K.G. Gopchandran, P. Koshy, V.K. Vaidyan, B. Joseph, Opt. Mater. 28 (2006) 1405.
[19] Powder Diffraction File, File No. 6-0413, JCPDS-International Center for Diffraction Data, Pennsylvania, 1972.
[20] V. Khranovskyy, U. Grossner, O. Nilsen, V. Lazorenko, G.V. Lashkarev, B.G. Svensson, R. Yakimova, Thin Solid Films 515 (2006) 472.
[21] X.D. Zhou, W. Huebner, Appl. Phys. Lett. 79 (2001) 3512.
[22] W.B. White, V.G. Keramidas, Spectrochim. Acta, Part A 28 (1972) 501.
[23] M. Rojas-Lopez, J. Nieto-Navarro, E. Rosendo, H. Navarro-Contreras, M.A. Vidal, Thin Solid Films 379 (2000) 1.
[24] A.G. Murillo, C.L. Luyer, C. Garapon, C. Dujardin, E. Bemstein, C. Pedrini, J. Mugnier, Opt. Mater. 19 (2002) 161.
[25] W.E. Lee, Y.-K. Fang, J.-J. Ho, C.-Y. Chen, L.-H. Chiou, S.-J. Wang, F. Dai, T. Heieh, R.-Y. Tsai, D. Huang, F.C. Ho, Solid State Electron 46 (2002) 477.
[26] H. Kim, C.M. Gilmore, J.S. Horwitz, A. Pique, H. Murata, G.P. Kushto, R. Schlof, Z.H. Kafafi, D.B. Chrisey, Appl. Phys. Lett. 76 (2000) 259.
[27] J.R. Bellingham, W.A. Phillips, C.J. Adkins, J. Phys.: Condens. Mater. 2 (1990) 6207.
[28] H. Kim, A. Pique, J.S. Horwitz, H. Mattoussi, H. Murata, Z.H. Kafafi, D.B. Chrisey, Appl. Phys. Lett. 74 (1999) 3444.
[29] D.Y. Ku, I.H. Kim, I. Lee, S.K. Lee, T.S. Lee, J.-h. Jeong, B. Cheong, Y.-J. Baik, W.M. Kim, Thin Solid Films 515 (2006) 1364.